Review | Received 12 December 2025; Revised 14 February 2026; Accepted 26 March 2026; Published 14 April 2026
https://doi.org/10.55092/am20260006

Laser additive manufacturing of metallic lattice structures: material-structure-property concept, and future perspective

Bo Sun[1,2], Shixun Zheng[3] , Haoyu Liu[4], Sharifah Fatmadiana Wan Muhamad Hatta[1,2], Binghua Yang[5], Zhaoji Zong[6] and Quanjin Ma[7,8,9,*]

[1] Department of Electrical Engineering, Faculty of Engineering, Universiti Malaya, Kuala Lumpur 50603, Malaysia
[2] Centre of Printable Electronics, Universiti Malaya, Kuala Lumpur 50630, Malaysia
[3] Department of Biomedical Engineering, Faculty of Engineering, Universiti Malaya, Kuala Lumpur 50603, Malaysia
[4] Department of Biochemistry, Faculty of Science, Universiti Malaya, Kuala Lumpur 50603, Malaysia
[5] School of Optical and Electronic Information, Huazhong University of Science and Technology, Wuhan 430074, China
[6] Institute of Advanced Studies, Universiti Malaya, Kuala Lumpur 50630, Malaysia
[7] Institute of Advanced Materials and Technology, Guangdong University of Technology, Guangzhou, 510006, China
[8] Faculty of Mechanical & Automotive Engineering Technology, Universiti Malaysia Pahang Al-Sultan Abdullah, Pekan 26600, Malaysia
[9] Centre for Advanced Composite Materials (CACM), Universiti Teknologi Malaysia (UTM), Johor 81310, Malaysia

* Correspondence author; E-mail: maquanjin@gdut.edu.cn.

Highlights:

- Laser processing parameters and thermal history are directly linked to defect formation and microstructural anisotropy in Ni- and Ti-based lattice systems.
- Functionally graded and TPMS architectures offer improved specific stiffness and energy absorption compared to conventional strut-based lattices.
- Node reinforcement strategies, particularly filleted geometries, effectively reduce stress concentration and significantly enhance fatigue resistance.
- Lattice-enabled heat exchangers and vibration isolation systems demonstrate enhanced heat transfer efficiency and frequency-selective attenuation.
- Machine learning-driven design optimization and standardized qualification frameworks are identified as key enablers for next-generation lattice manufacturing.

Abstract: Metallic lattice structures have emerged as revolutionary lightweight materials with exceptional specific strength and multifunctional capabilities, particularly in aerospace applications.

This review comprehensively examines the state of the art in laser additive manufacturing (LAM) of metallic lattice structures, focusing on selective laser melting (SLM) and electron beam melting (EBM). We critically analyze recent advances in materials development, including nickel-based superalloys (GH4169/IN718, K465), titanium alloys (Ti-6Al-4V), and functionally graded composites. The review addresses key design considerations, including unit cell topology optimization, node reinforcement strategies, and gradient structures. We examine mechanical properties under various loading conditions, thermal management capabilities, and failure mechanisms through both experimental and numerical perspectives. Advanced detection methods, including micro-CT imaging and AI-based defect identification, are evaluated for quality assurance. Critical challenges, including surface roughness control, residual stress management, and size limitations, are discussed alongside emerging opportunities in machine-learning-assisted design and multi-material systems. This review provides essential insights for researchers and engineers seeking to advance lattice-structured applications in next-generation aerospace systems.

Keywords: lattice structures; additive manufacturing; selective laser melting; mechanical properties; aerospace applications; non-destructive testing

1. Introduction

The growing demand for structural efficiency and multifunctional performance across engineering sectors, including aerospace, automotive, energy, and biomedical applications, has driven the development of metallic lattice structures as advanced lightweight systems [1,2]. These periodic cellular architectures offer unprecedented combinations of specific strength, stiffness, and energy absorption, while enabling integrated thermal management and vibration-damping capabilities [3,4]. Their architected nature allows mechanical performance to be tailored through topology, relative density, and geometric hierarchy. The emergence of laser additive manufacturing (LAM) technologies, particularly selective laser melting (SLM) and electron beam melting (EBM), has revolutionized the fabrication of these complex geometries, overcoming the limitations of traditional manufacturing methods [5,6]. Unlike conventional subtractive or casting-based processes, LAM allows the direct fabrication of complex, interconnected geometries without tooling constraints. The layer-wise manufacturing approach enables precise control over strut dimensions, node geometry, and internal architecture at the microscale.

Furthermore, the localized and controllable thermal input during laser processing provides opportunities to tailor microstructure, relative density, and defect distribution. These unique capabilities make LAM particularly suitable for realizing architected metallic lattices with design-driven mechanical and multifunctional performance. Recent advances in LAM have enabled the production of lattice structures with feature sizes ranging from hundreds of micrometers to several millimeters, achieving relative densities as low as 0.01% [7]. This capability has opened new design spaces for aerospace applications, including turbine blades, heat exchangers, impact-resistant panels, and morphing structures [8,9]. The global aerospace additive manufacturing market, valued at $3.2 billion in 2023, is projected to reach $9.8 billion by 2030, with lattice structures representing a significant growth segment [10].

Despite these advances, several critical challenges remain. The formation mechanisms of defects during laser-matter interaction, particularly in high-temperature alloys, are not fully understood [11]. The relationship between processing parameters, microstructure evolution, and mechanical properties

requires further elucidation [12]. Additionally, the lack of standardized testing methods and qualification procedures hinders industrial adoption [13]. This review systematically examines the state-of-the-art across the full technology spectrum: Section 2 covers key metallic materials and their AM-specific behaviors; Section 3 discusses design methodologies from unit cells to hierarchical structures; Sections 4–5 examine manufacturing processes and resulting mechanical properties; Section 6 highlights thermal and multifunctional capabilities; Sections 7–8 address modeling approaches and quality assurance; Section 9 presents industrial applications; and Sections 10–11 identify challenges and future research directions. While this review focuses primarily on SLM, we also include relevant advances in EBM, given its complementary role in lattice fabrication, and briefly acknowledge other metallic AM processes as relevant to lattice structures. A schematic overview of the topics covered in this review is presented in Figure 1.

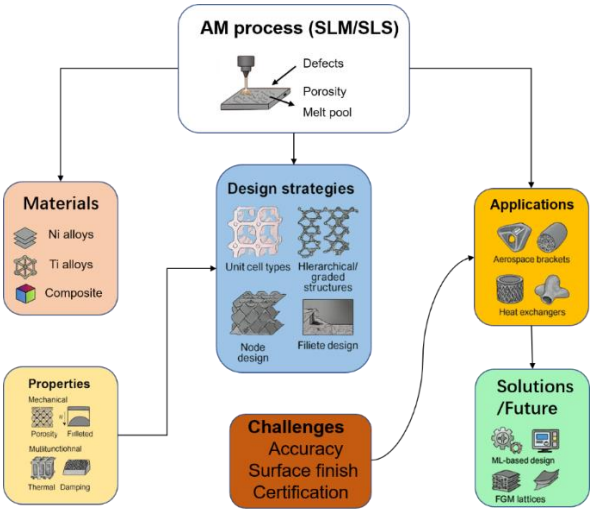

Figure 1. Schematic overview of metallic lattice structures fabricated via laser-based additive manufacturing (SLM/SLS). The flow begins with material selection, proceeds through key design strategies, and culminates in the AM process.

2. Materials for lattice structures

2.1. Nickel-based superalloys

Nickel-based superalloys are widely used in high-temperature structural applications, including aerospace turbines and energy systems, due to their exceptional creep resistance and oxidation stability [14]. GH4169 (Inconel 718), containing 50%–55% Ni, 17%–21% Cr, and strengthened by γ' ($Ni_3(Al,Ti)$) and γ'' (Ni_3Nb) precipitates, exhibits excellent processability via SLM [15]. Recent studies by Zhang, Sun [16] demonstrated that optimized scanning strategies with alternating stripe patterns reduce residual stress by 45% while maintaining relative density above 99.5%. The solidification behavior during SLM processing significantly influences the microstructure. Chen, Clark [17] revealed through *in-situ* synchrotron X-ray imaging that the cooling rate of 10^6–10^7 K/s promotes the columnar-to-equiaxed transition, thereby affecting the formation of Laves phase and carbides. Post-processing heat treatment at 980 ℃ for 1 hour followed by double ageing (720 ℃/8 h + 620 ℃/8 h) optimizes the γ''/γ' precipitation, achieving tensile strength exceeding 1400 MPa [18].

The stress concentration reduction mechanism in filleted nodes occurs through gradual load transfer and the elimination of sharp stress risers, where the smooth radius distributes stress over a larger area, preventing crack initiation at angular intersections. The microstructure of SLM-fabricated IN718 lattices was shown in Figure 2: (a) as-built (with dendritic/cellular structures and Laves phases) *versus* (b–d) after various heat treatments, illustrating grain refinement and precipitate evolution. These images vividly demonstrate how post-processing alters the microstructure (e.g., dissolution of Laves phase and precipitation of γ′/γ″) to improve mechanical performance.

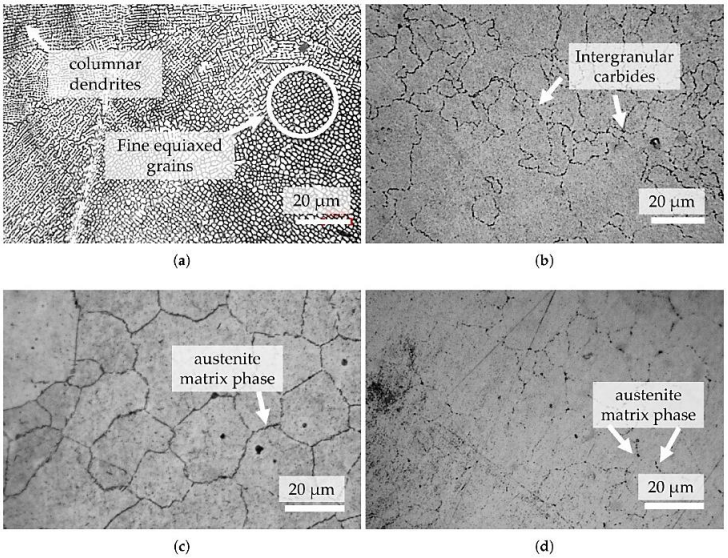

Figure 2. Microstructural characterization of SLM IN718 with various heat treatments. **(a)** As-built sample (nHT); **(b)** HT1; **(c)** HT2; **(d)** HT3 [19].

IN718 lattice structures produced by SLM show cellular dendritic growth with Laves phase formation in the as-built state, contributing to brittleness. Post-processing heat treatments dissolve the Laves phase and promote the precipitation of γ′/γ″ phases, thereby enhancing strength and ductility. K465 superalloy presents unique challenges due to its high Al+Ti content (>7 wt %), which increases the susceptibility to solidification cracking [20]. Recent work by Liu, Wang [21] demonstrated that preheating the substrate to 800 ℃ and employing a chessboard scanning strategy with a 67 ° rotation between layers significantly reduces crack density from 2.5 mm/mm ²to 0.3 mm/mm ².

2.2. Titanium alloys

Ti-6Al-4V is a widely used alloy in lightweight structural lattice applications, including aerospace components, biomedical implants, and automotive systems, owing to its high strength-to-weight ratio and biocompatibility [22]. The α+β microstructure evolution during SLM processing follows a complex pathway: β solidification → martensitic transformation → α' decomposition during intrinsic heat treatment [23]. Wang, Yang [24] demonstrated that controlling the volumetric energy density (VED = P/(v × h × t)) between 40–60 J/mm ³ optimizes the balance between density and microstructure refinement. The fabricated gear's body is a lattice structure optimized via topology optimization (as shown in Figure 3), and the image shows the successful build, including the teeth, hub, and internal lattice. Figure 3 highlights that the supporting structures and surface finish are managed on a complex geometry.

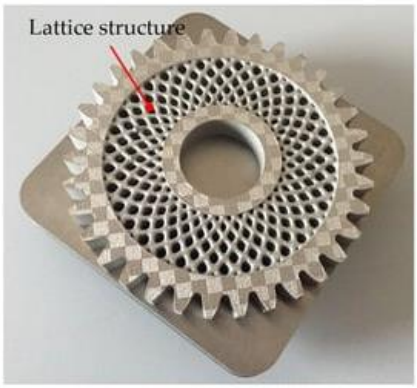

Figure 3. Illustration of a lightweight Ti-6Al-4V lattice gear produced by SLM [25].

Lattice structures integrated into mechanical components, such as gears, enable substantial mass reduction without compromising strength. The example shown demonstrates how topology optimization can embed a lightweight Ti6Al4V lattice core within a functional gear, suitable for aerospace or automotive applications. Recent advances in alloy design have led to the development of Ti-Al-V-Mo systems with enhanced strength. The addition of 2% Mo promotes β-phase stability, resulting in improved ductility without compromising strength [26]. Furthermore, the incorporation of boron (0.1 wt %) as a grain refiner reduces the prior β grain size from 150 μm to 45 μm, enhancing fatigue resistance [27]. Process anisotropy considerations are critical, as build orientation affects both the α/β phase distribution and mechanical properties, with vertical builds typically showing 10%–15% higher strength but reduced ductility compared to horizontal orientations due to alignment of the columnar grain structure.

2.3. Functionally graded and composite materials

The integration of reinforcement phases offers pathways to enhanced performance. TiB_2/IN718 composites, produced through *in-situ* reaction during SLM, exhibit 25% higher yield strength compared to unreinforced IN718 [28]. The TiB_2 particles (50–200 nm) act as heterogeneous nucleation sites, refining the grain structure and providing Orowan strengthening [29]. Recent developments in multi-material LAM enable spatial variation in lattice composition. Li *et al.* demonstrated gradient structures transitioning from 316L stainless steel to Inconel 625, achieving tailored thermal expansion coefficients for thermal management applications [30]. The interface region, characterized by a 200 μm transition zone, exhibits no detrimental intermetallic formation when processed with optimized interlayer dwell time [31].

3. Design methodologies

3.1. Unit cell topology

The selection of unit cell topology profoundly influences mechanical behavior. Beyond traditional designs (BCC, FCC, octet), triply periodic minimal surfaces (TPMS) have emerged as superior architectures [32]. Gyroid structures exhibit 40% higher energy absorption than equivalent-density strut-based designs due to their smooth stress distribution and absence of stress concentrations [33]. A practical design consideration is powder removal accessibility-TPMS structures like gyroids may trap unsintered powder in closed cells,

necessitating drain holes or post-processing techniques such as chemical dissolution or ultrasonic cleaning to ensure complete powder extraction.

Various lattice unit cells, including BCC, FCC, octet, and gyroid topologies, offer distinct geometric connectivity and deformation mechanisms. Strut-based lattices, such as BCC and octet lattices, are easier to design and analyze but may suffer from stress concentration at nodes. Conversely, TPMS-based lattices, such as the gyroid, offer smoother stress distribution due to their continuous surfaces, thereby enhancing mechanical performance and manufacturability. Diamond, gyroid, BCC and I-WP structures are shown in Figure 4 at equal scale and relative density (~50% porosity). It visually compares traditional strut-based lattices to smooth-surface TPMS lattices. The gyroid and diamond have continuous surfaces, whereas the BCC has sharp nodes. Minimal surface structures such as the gyroid, diamond, primitive, and I-WP have attracted attention for their excellent surface continuity and manufacturability via AM. Compared to strut-based lattices, these topologies exhibit smoother profiles and reduced stress concentrations. Recent topology optimization approaches integrating machine learning with finite element analysis. Zhang, Song [34] employed convolutional neural networks to predict mechanical properties of novel unit cells, reducing design iteration time by 85%. The optimization considers multiple objectives: maximizing stiffness, minimizing weight, and ensuring manufacturability constraints (minimum feature size, overhang angles) [35].

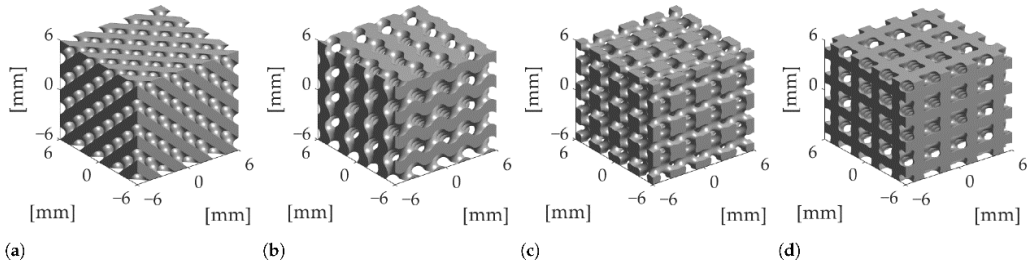

Figure 4. CAD representations of various lattice unit cell designs, including **(a)** diamond (Schwarz D minimal surface); **(b)** gyroid (TPMS); **(c)** BCC strut lattice; **(d)** I-WP minimal surface. These topologies differ in connectivity and deformation behavior, thereby influencing the mechanical response, energy absorption, and manufacturability of AM lattice structures.

3.2. Gradient and hierarchical structures

Nature-inspired gradient designs offer superior performance compared to uniform structures. Density gradients following power-law distributions ($\rho(z) = \rho_0(z/H)^n$) optimize stress distribution under compression, increasing energy absorption by 60% [36]. The gradient exponent n = 0.5–0.7 provides optimal balance between strength and deformation stability [37]. Hierarchical designs incorporating multiple length scales enhance mechanical properties through structural hierarchy. Second-order lattices, where struts themselves possess lattice architecture, achieve specific stiffness exceeding theoretical bounds for first-order structures [38]. The critical aspect ratio for second-order struts (L/D > 15) prevents premature buckling while maintaining weight efficiency [39].

A first-order lattice (octet) is shown in Figure 5 alongside a second-order lattice where a miniature lattice of the same type replaces each strut of the octet. The figure illustrates the concept of hierarchical (multi-scale) design: the “lattice of lattices” architecture. To improve stiffness and energy absorption, hierarchical lattice architectures have been proposed, in which each primary strut is substituted with a secondary lattice. This nested approach draws inspiration from biological structures such as bone or

bamboo, combining mechanical efficiency with low density. Graded TPMS structures enable tailored properties but introduce challenges in printability, especially where wall thickness is minimized. Thin regions are more prone to surface roughness and geometric deviation due to inadequate heat dissipation and structural support during printing.

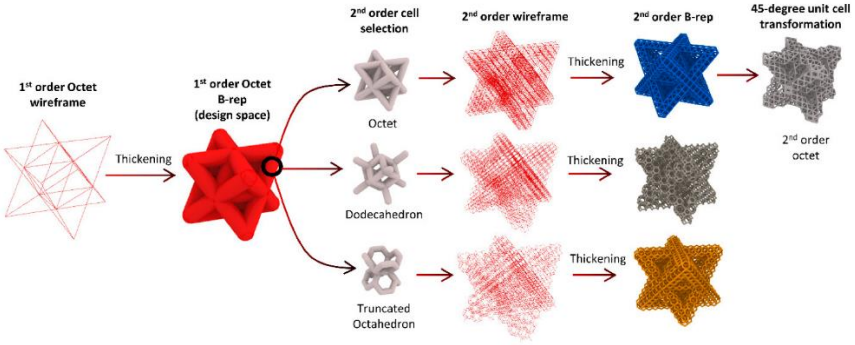

Figure 5. Schematic representation of a hierarchical lattice structure, where primary struts of a first-order octet lattice are replaced with secondary lattices, enhancing energy absorption and stiffness while maintaining lightweight characteristics. Such designs mimic natural hierarchical architectures [40].

3.3. Node reinforcement strategies

Node geometry plays a decisive role in failure initiation in lattice structures, as stress concentration typically localizes at strut intersections. Finite element analysis indicates that sharp node corners can generate stress concentration factors exceeding 3.5 under compressive or cyclic loading [41]. These sharp intersections act as crack initiation sites due to abrupt changes in load path direction and bending-dominated stress accumulation. Filleted nodes with radius r = 0.15D–0.20D (where D is strut diameter) reduce stress concentration by 45% while increasing fatigue life by an order of magnitude [42]. The improvement in yield strength with increasing fillet radius is plotted in Figure 6. The images in Figure 6 visually confirm that FEA results show stress concentration factors > 3.5 at sharp corners and state that r = 0.15D–0.2D fillets greatly extend fatigue life, showing where cracks would initiate and how fillets alleviate them.

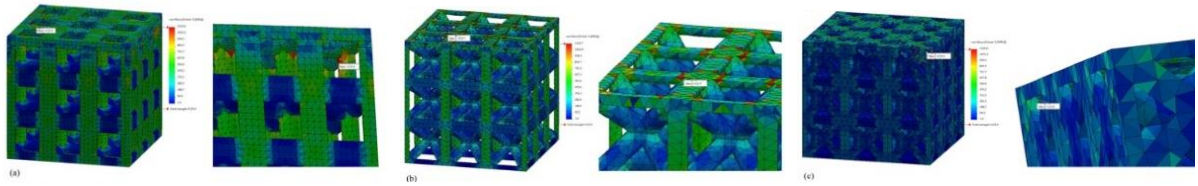

Figure 6. Finite element analysis showing von Mises stress distributions in lattice nodes: **(a)** sharp node corners generate significant stress concentrations; **(b)** filleted nodes (radius ≈ 0.15D) effectively mitigate stress concentration; **(c)** face-centered cubic. Node smoothing improves fatigue resistance and structural reliability [43].

Sharp lattice nodes can lead to stress localization and premature failure under cyclic loading. Filleting these nodes (e.g., using a radius of 0.15D–0.2D) redistributes stress more uniformly, thereby improving fatigue resistance and yield strength. FEA simulations have validated this stress-reduction

strategy. Advanced node designs incorporate variable thickness and material composition. Beyond geometric smoothing, advanced node reinforcement strategies include selective node thickening and localized material strengthening. Increasing laser power by approximately 30% at node regions enhances local density and microstructural refinement without significantly increasing overall weight [44]. This approach, termed "functional grading at microscale", represents a paradigm shift in lattice design [45].

4. Manufacturing process optimization

4.1. Process parameters

The complex interplay between laser parameters determines final part quality. Recent high-speed imaging studies (10,000 fps) reveal melt pool dynamics governing defect formation [46]. The dimensionless number $\Pi = (P \cdot \eta)/(v \cdot \lambda \cdot \Delta T)$ (where η is the absorption coefficient, λ is thermal conductivity, and ΔT is the melting temperature) provides a universal framework for parameter selection across materials [47]. Layer thickness optimization balances productivity and quality. Thin layers (20–30 μm) improve surface quality but increase build time and thermal cycling. Adaptive layer thickness, varying from 20 μm for fine features to 60 μm for bulk regions, reduces build time by 40% while maintaining quality [48].

4.2. Support structure design

Support structures for lattice components require careful consideration. Tree-like supports with gradual diameter reduction (following $D(h) = D_0(1-h/H)^{0.5}$) minimize material usage while ensuring stability [49]. The support-part interface, designed with a 0.3–0.5 mm offset, facilitates removal without surface damage [50]. Self-supporting lattice designs eliminate the need for external supports through geometric constraints. Maintaining strut angles > 35 ° from the horizontal and incorporating gradual transitions prevent collapse during construction [51]. This approach reduces post-processing time by 60% and material waste by 40% [52].

4.3. In-situ monitoring and control

Real-time process monitoring enables adaptive control for consistent quality. Acoustic emission sensors detect cracking events with 95% accuracy, enabling immediate parameter adjustment [53]. Pyrometry-based melt pool monitoring maintains temperature within ± 50 ℃ through closed-loop power control [54]. Machine learning algorithms trained on multi-sensor data predict defect formation with 92% accuracy. Integration of these systems with adaptive slicing software creates "intelligent" AM systems capable of self-optimization [55], which represents the future of quality assurance in LAM [56].

4.4. SLM versus EBM process considerations

Selective laser melting and electron beam melting offer complementary advantages for lattice fabrication. EBM's higher build temperature (700 ℃–1000 ℃) and vacuum environment result in lower residual stresses and often eliminate the need for stress relief heat treatment, particularly beneficial for high-temperature alloys [57]. However, EBM's larger beam size (0.1–0.2 mm *vs* 0.02–0.1 mm for SLM)

produces rougher surface finishes (Ra = 25–40 μm) and limits minimum feature resolution. SLM offers superior dimensional accuracy and broader material compatibility, but requires careful management of residual stresses through process optimization or post-processing. For lattice structures, EBM excels at larger features where surface finish is secondary, while SLM enables fine-featured designs that require high precision.

5. Mechanical properties and performance

5.1. Quasi-static behavior

The compressive behavior of lattice structures exhibits three distinct regimes: linear elastic, plateau, and densification [58]. The Gibson-Ashby scaling relationships ($E^*/Es = C_1(\rho^*/\rho s)^n$) provide first-order approximations but fail to capture size effects and manufacturing defects [59]. These deviations occur because the Gibson-Ashby theory assumes perfect cellular geometry and bulk material properties in struts, whereas AM lattices exhibit geometric imperfections, surface roughness, and size-dependent material behavior. Struts with diameters below 500 μm exhibit significant deviations from bulk properties due to surface-area-to-volume effects and defect populations.

These images in Figure 7 capture the collapse mechanisms, e.g. layer-by-layer buckling in a cubic lattice *vs* diagonal shear in an octahedron—just before failure. Recent experimental studies using digital image correlation (DIC) reveal strain localization patterns that precede macroscopic failure. Shear bands initiate at 45 °to the loading direction in BCC lattices, while face-centered designs exhibit layer-by-layer collapse [60]. The critical strain for shear band formation correlates with the lattice connectivity (Z = 6 for BCC, Z = 12 for FCC) [61].

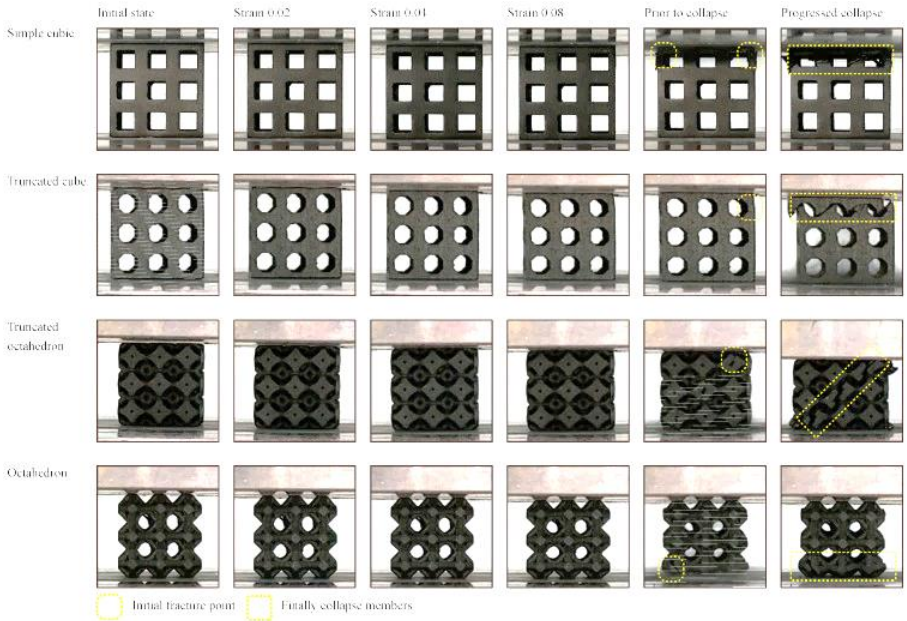

Figure 7. Sequential photographs of lattice specimens under compression for several unit cell types (simple cubic, octahedral, *etc.*), all at 30% relative density [43].

As for the deformation modes, all the specimens used in the experiments showed the same deformation modes. Figure 8 presents the deformation evolution of lattice blocks with varying cell sizes under

quasi-static compression. Across all specimens, deformation localization consistently initiates near the mid-height of the blocks in the sequential images. This characteristic mid-plane localization indicates a bending-dominated behavior, in which strut members aligned with the loading direction undergo progressive buckling (visible as lateral bowing in the images) before global densification. The formation of these deformation bands stems from geometric instability and load redistribution driven by connectivity. In lower-connectivity lattices, the load-transfer path is less redundant, leading to stress concentration in the central layers and triggering early shear-dominated collapse. As compression proceeds to $\varepsilon = 0.3–0.4$, densification becomes pronounced, characterized by visually distinct strut interlocking and local compaction, which enhances energy absorption. Notably, smaller cell sizes exhibit slightly more uniform deformation patterns, attributed to increased nodal constraint and a reduced effective slenderness ratio of the struts. Collectively, these observations suggest that deformation localization is governed not merely by initial imperfections or residual stresses, but fundamentally by intrinsic topological connectivity and strut slenderness. Thus, the transition in deformation modes is strongly architecture-dependent rather than purely defect-driven.

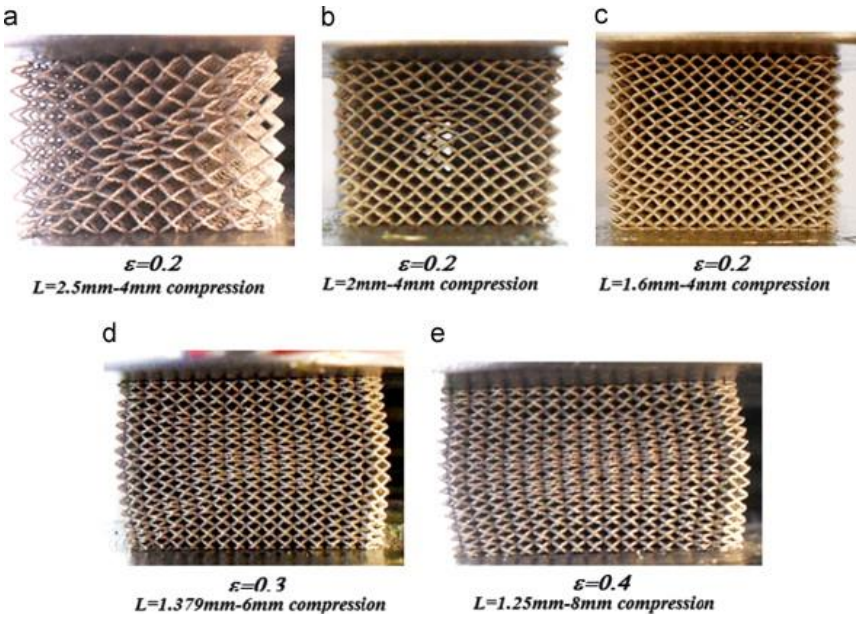

Figure 8. Deformation modes of lattice blocks for certain deformation amounts [60]. Reprinted with permission. Copyright 2013 Elsevier.

Figure 9 compares experimental and finite element (FE) stress-strain responses for lattice structures with cell sizes of 2.5 mm and 1.25 mm. For the 2.5 mm cell, both the beam and solid FE models accurately capture the initial stiffness, peak strength, and overall loading path observed in experiments. However, for the 1.25 mm cell, the solid model closely aligns with the experimental response, whereas the beam model underestimates the strength. Specifically, the beam model correctly predicts the initial stiffness but yields approximately 10% lower strength than measured experimentally. This discrepancy is primarily due to the beam elements' inability to represent the complex geometry at the strut junctions fully. Additionally, surface irregularities such as variable strut diameters and partially melted powder residues may further influence the mechanical performance of micro-lattice structures, which the simplified beam model cannot account for.

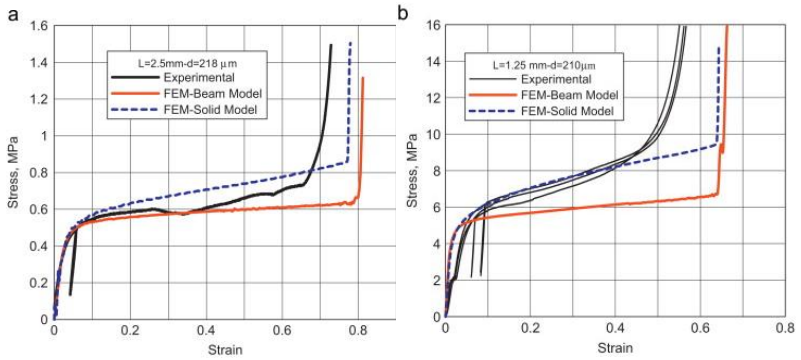

Figure 9. Comparisons of numerical and experimental compression results for: **(a)** 2.5 mm; **(b)** 1.25 mm cell size micro lattice blocks. L: the unit cell size, d: the strut diameter [60]. Reprinted with permission. Copyright 2013 Elsevier.

5.2. Dynamic and impact response

High strain rate behavior ($\dot{\varepsilon} > 10^3 s^{-1}$) differs significantly from quasi-static response due to inertial effects and strain rate sensitivity [62]. Split-Hopkinson pressure bar tests reveal 30%–50% strength enhancement at high rates for Ti-6Al-4V lattices [63]. The dynamic strength enhancement factor follows $\beta = 1 + (\dot{\varepsilon}/\dot{\varepsilon}_0)^m$, where m = 0.02−0.03 for titanium alloys [64]. Blast-resistance studies using explosive loading demonstrate the superior performance of gradient structures. The impedance mismatch between layers promotes stress wave attenuation, reducing transmitted impulse by 40% compared to uniform designs [65]. Sacrificial layers with programmed failure enhance protection while maintaining structural integrity [66].

5.3. Fatigue and fracture

Fatigue behavior remains a critical concern for aerospace applications. S-N curves for SLM lattices show 50%–70% reduction in fatigue strength compared to bulk material due to surface defects and residual stress [67]. Surface treatments, including electropolishing and shot peening, improve fatigue life by 3–5 times [68]. Fracture mechanics approaches reveal the mechanisms of crack propagation. The Paris law exponent (m = 3.5–4.5) for lattice structures exceeds bulk values due to mixed-mode loading and stress redistribution [69]. Crack deflection at cell boundaries provides extrinsic toughening, increasing fracture toughness by 25% [70]. Build orientation significantly affects fatigue anisotropy, with vertically built specimens showing 20%–30% longer fatigue life due to favorable crack propagation paths at layer interfaces. Property scatter in AM lattices is typically 2–3 times higher than in bulk materials due to manufacturing variability, requiring statistical design approaches and larger safety factors.

6. Thermal and multifunctional properties

6.1. Thermal management

Lattice structures offer unique thermal management capabilities through combined conduction and convection [71]. Forced convection through Kagome lattices yields heat transfer coefficients of 500–800 W/m²K, comparable to those of conventional heat sinks at 50% lower weight [72]. Depicted

here are devices fabricated using our in-house AM system and control software (Figure 10), which were also cut in half to measure the gyroid structures and their quality. The findings confirmed that the printed aluminum HX exhibited no water leakage into adjacent channels.

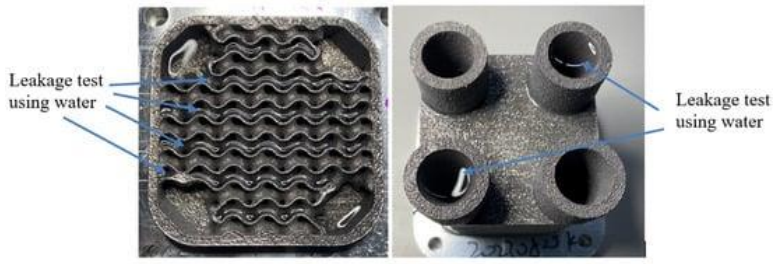

Figure 10. The photograph of a 3D-printed gyroid heat exchanger core [73].

As illustrated in Figure 11, the performance of the HX-70 was compared with that of the commercial heat exchanger (HX) model BT3 × 8–20. Specifically, for a 3 × 3 × 3 inch ^{3}gyroid HX (HX70–555, featuring a 0.3 mm wall thickness and 5 mm gyroid unit length), the comparison with a commercial 20 kW plate HX (BT3 × 8–20, dimensions 3 × 8 × 2.2 inch ^{3}) at the same flow rate revealed a twofold size reduction, a two-to-threefold decrease in pressure drop, and a two-to-threefold enhancement in heat transfer coefficient. These exceptional characteristics distinguish the TPMS HX and warrant further in-depth research. The effective thermal conductivity is calculated using modified Maxwell-Eucken models that account for strut orientation and connectivity. Anisotropic designs with preferential strut alignment enhance directional heat transfer by 200% [74]. Integration of heat pipes into struts creates active thermal management systems for high-heat-flux applications [75].

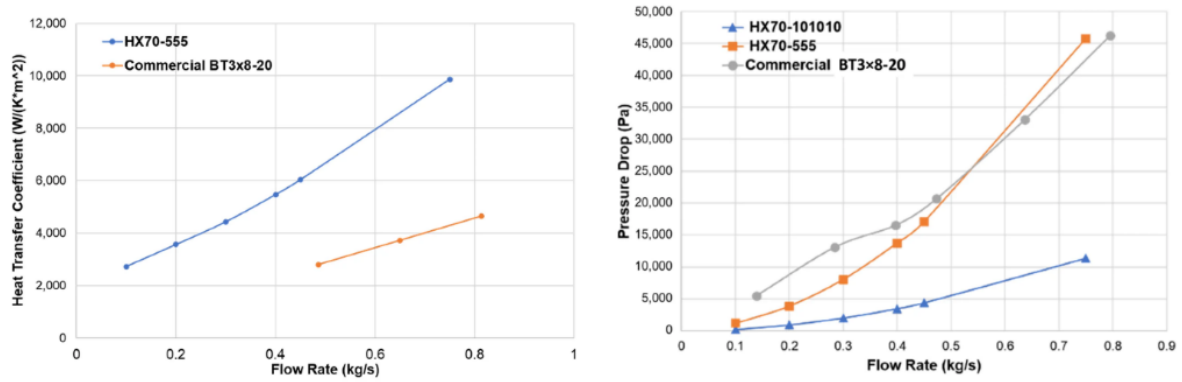

Figure 11. Comparisons of the gyroid lattice HX and conventional finned heat exchanger performance [73].

6.2. Vibration damping

The cellular architecture provides inherent damping through multiple mechanisms: material damping, air pumping, and friction at nodes [76]. Loss factors (η = 0.01–0.05) exceed bulk material values by an order of magnitude [77]. Viscoelastic coatings on struts further enhance damping without a significant weight penalty [78]. Phononic bandgap engineering enables frequency-selective vibration isolation. Periodic variation in unit cell size creates bandgaps at targeted frequencies, achieving 30 dB attenuation in specific frequency ranges [79]. This capability enables simultaneous load bearing and vibration

isolation [80]. Figure 12 provides a concrete example of such a lattice meta-material, supporting the concept that lattice structures can be engineered for specific vibrational properties.

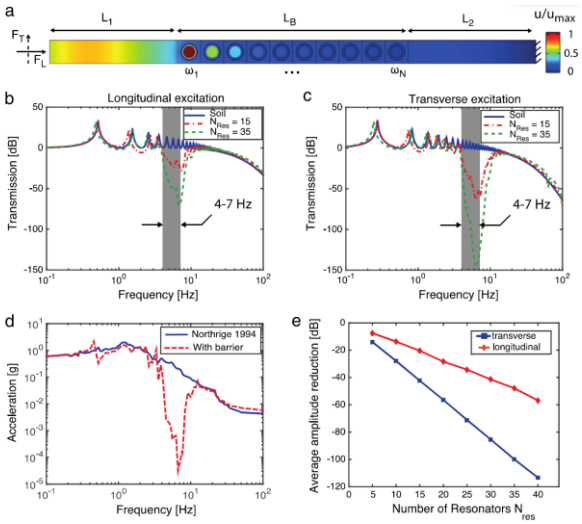

Figure 12. The lattice layout and the mechanism for damping vibrations. **(a)** The color intensity represents the normalized displacement amplitude, with vibration localized around resonator ω_1 in this instance. **(b)** presents the transmission spectrum for longitudinal waves (FT = 0) across different numbers of resonators (0, 15, and 35), while **(c)** shows the transmission spectrum for transverse excitations (FL = 0). To demonstrate the potential filtering effect on the spectrum of a real earthquake, **(d)** applies the transfer function with 35 resonators to the 1994 Northridge earthquake, earthquake recording data is available for download from the PEER Ground Motion Database. **(e)** provides a design guideline that illustrates the average attenuation as a function of the number of resonators in the array [78]. Reprinted with permission. Copyright 2015 Elsevier.

7. Numerical modeling and simulation

7.1. Multiscale modeling approaches

Accurate prediction of lattice behavior requires multiscale modeling spanning from microstructure to structure [81]. Crystal plasticity finite element models capture microscale deformation mechanisms, including slip-system activation and grain-boundary effects [82]. Homogenization techniques bridge micro-macro scales, reducing computational cost by 10 ^{3}while maintaining 95% accuracy [83]. Recent advances in neural network-based constitutive models capture complex path-dependent behavior. Physics-informed neural networks (PINNs) trained on limited experimental data predict stress-strain response with $R^2 > 0.98$ [84]. These models enable rapid design optimization without extensive experimental campaigns [85].

7.2. Process simulation

Thermal–mechanical process simulation plays a critical role in predicting residual stress and geometric distortion in lattice structures, where thin struts and node intersections are particularly susceptible to deformation. The inherent strain method, calibrated through neutron diffraction measurements, has been applied to complex lattice geometries and achieves prediction accuracy within 15% [86]. In lattice

architectures, residual stress accumulation can lead to strut bending, dimensional deviation, and node cracking, which are more pronounced than in bulk components due to reduced cross-sectional area. Incorporating phase transformation kinetics improves predictions for materials undergoing solid-state transformations [87]. Melt-pool dynamics simulation using computational fluid dynamics reveals keyhole-formation mechanisms [88]. Excessive power density may induce localized keyhole porosity, which is particularly detrimental in slender lattice struts [89].

8. Detection and quality control methods

8.1. Non-destructive testing

X-ray computed tomography (CT) remains the gold standard for detecting internal defects. High-resolution micro-CT (voxel size < 5 μm) reveals pore morphology, size distribution, and location with 98% detection rate for pores > 50 μm [90]. Recent advances in helical CT reduce scan time by 75% while maintaining resolution [91]. Automated defect recognition using convolutional neural networks achieves 99.5% classification accuracy for common defect types (lack of fusion, keyhole porosity, cracks) [92]. Integration with digital twins enables predictive quality control, enabling identification of high-risk regions before manufacturing [93].

Non-destructive inspection plays a critical role in evaluating internal defects and dimensional fidelity in lattice structures fabricated by L-PBF. As illustrated in Figure 13, micro-CT scans provide detailed insight into internal pore distribution, geometric deviations, and crack formation. The highlighted CT reconstruction of TPMS lattices shows a clear mismatch between the printed structure and its CAD model, with color-coded deviation maps quantifying regional discrepancies. Pores and irregularities are visibly concentrated along strut intersections, a common site for thermal accumulation and insufficient fusion. The observed deviations in wall thickness up to ±0.20 mm demonstrate the sensitivity of CT for capturing fine-scale manufacturing errors. Such internal defects, including lack-of-fusion voids and surface-connected cracks, cannot be detected solely by surface imaging. These results support the growing use of CT-based *in-situ* validation workflows and digital twins for real-time quality assurance and predictive defect mitigation in metallic lattice fabrication.

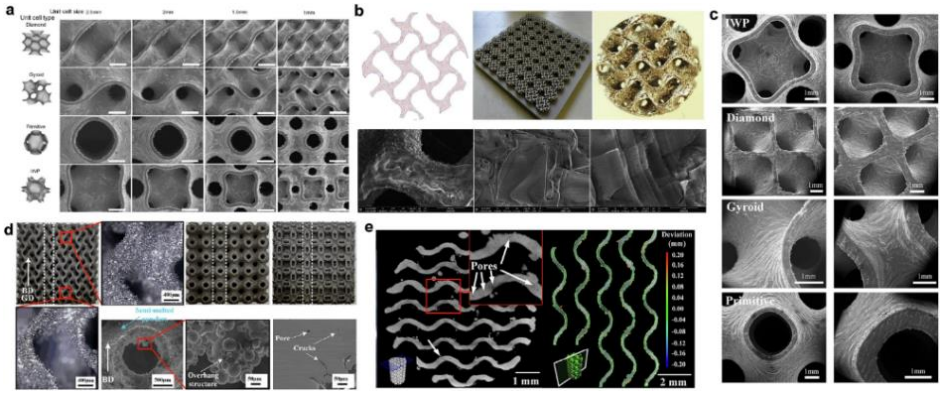

Figure 13. Micro-CT-based evaluation of TPMS lattice structures: **(a–d)** SEM and CT images highlighting typical defects such as partially melted powder, surface roughness, cracks, and overhang-induced irregularities; **(e)** comparison of CT reconstruction *vs* CAD geometry, showing pore formation and dimensional deviations (quantified by color-coded deviation map) [94]. Reprinted with permission. Copyright 2025 Springer Nature.

8.2. In-situ monitoring

In-situ monitoring is particularly important for lattice fabrication because thin struts and complex node geometries are sensitive to thermal instability. Layer-wise imaging with high-resolution cameras (>5 megapixels) enables real-time detection of surface irregularities that may affect strut diameter uniformity and node connectivity. Machine vision algorithms can identify anomalies such as recoater interference, localized overmelting, and incomplete fusion, which are especially detrimental in fine-lattice architectures [95]. Thermographic monitoring reveals hot spots indicative of overheating or incomplete fusion [96]. Given the reduced cross-sectional area in lattice members, even minor thermal fluctuations can lead to dimensional deviations or micro-porosity. Acoustic emission monitoring further enables crack detection during fabrication, with characteristic frequency signatures associated with strut fracture or node-level cracking (100–400 kHz). Wavelet-based signal processing helps distinguish lattice-specific defect signals from background machine noise [97]. These monitoring approaches are therefore critical for ensuring geometric fidelity and mechanical reliability in lattice structures.

8.3. Mechanical testing standards

Standardization efforts by ASTM and ISO provide testing guidelines for lattice structures. ASTM F3575–23 specifies compression testing procedures, including specimen geometry (minimum 5 × 5 × 5 unit cells) and loading rates [43]. However, size effects and boundary conditions significantly influence measured properties, necessitating careful interpretation [98]. Novel testing methods address lattice-specific challenges. Micro-mechanical testing using nanoindentation reveals strut-level properties, accounting for size effects and surface conditions [99]. Digital volume correlation enables full-field strain measurement during loading, validating numerical models [100].

8.4. Post-processing and final quality assurance

Hot isostatic pressing (HIP) is widely employed to eliminate internal porosity and improve fatigue performance, typically conducted at 920 ℃ and 100 MPa for Ti-6Al-4V lattices, achieving > 99.8% density. Surface finishing presents unique challenges for lattice structures due to limited accessibility. Chemical etching using HF/HNO_3 solutions can reduce surface roughness from 15–20 μm to 8–12 μm, but requires careful control to prevent strut thinning. Electropolishing offers selective surface improvement but is limited to accessible surfaces. These post-processing steps are often mandatory for flight-critical applications.

9. Applications and case studies

9.1. Aerospace structures

Boeing's implementation of Ti-6Al-4V lattice brackets in the 787 Dreamliner achieved 50% weight reduction while meeting stringent safety requirements [101]. The optimized topology, combining solid skins with graded lattice cores, withstands a 150% design load with a factor of safety exceeding 1.5 [102]. Qualification involved extensive fatigue testing under simulated flight loads, with the lattice bracket demonstrating 2 million cycles at 120% design load without failure. The certification process required developing new test protocols since traditional design allowables for bulk materials do not apply to

complex lattice geometries, necessitating component-level qualification. Airbus's development of lattice-based heat exchangers for next-generation aircraft demonstrates multifunctional integration. The Gyroid-based design achieves a 200% higher heat transfer rate per unit weight than conventional plate-fin designs [103,104]. Successful flight tests validate performance under extreme conditions (−55 ℃ to 120 ℃, 9 g acceleration) [105].

9.2. Propulsion systems

GE Aviation has demonstrated the potential of additive manufacturing to integrate complex lattice cooling channels within turbine blades, structures that are nearly impossible to achieve with conventional methods. These lattices, characterized by high porosity, low weight, and excellent strength, markedly enhance cooling efficiency without compromising mechanical performance [106]. Studies indicate that optimized lattice channels can reduce blade temperatures by 100 ℃–150 ℃, thereby alleviating thermal stress, mitigating fatigue damage, and extending service life by 20%–30% or more [106]. Furthermore, multi-objective optimization of lattice geometries, including parameters such as height, diameter, and inclination, enables a balanced Improvement in heat transfer, structural strength, and vibration resistance, highlighting the multifunctional advantages of lattice-enabled cooling designs.

In the SpaceX Raptor engine, SLM has enabled the fabrication of Inconel 718 lattice structures that integrate cooling channels directly within the load-bearing chamber walls, designs unattainable by conventional methods. These lattice channels significantly enhance heat transfer by improving coolant distribution and localized vortex formation, while simultaneously reducing weight by ~30% without compromising strength [107,108]. Combining high-temperature capability, corrosion resistance, and design flexibility, SLM-produced Inconel 718 lattices represent a key technology for achieving lightweight, integrated thermal management in aerospace propulsion systems.

9.3. Space applications

NASA and other research initiatives are exploring multilayer, lightweight structures, such as Whipple shields, for protecting lunar habitats from micrometeoroid impacts. A key emerging trend is the integration of gradient lattice or quasi-lattice cores into protective layers to balance extreme impact resistance with weight reduction. Numerical and experimental studies show that sandwich panels incorporating body-centered cubic (BCC) lattices can achieve significantly higher resistance to hypervelocity projectiles (2–6 km/s) than traditional Whipple shields at equal areal density, while gradient lattice cores offer further optimization of energy dissipation pathways, enabling effective interception at velocities up to 7 km/s [109,110]. Beyond impact resistance, these multilayer lattice hybrids also provide thermal insulation, which is critical for mitigating the extreme lunar temperature cycle. Importantly, the realization of such complex architectures increasingly relies on additive manufacturing, which enables the precise fabrication of tailored lattice geometries and facilitates the use of both *in-situ* resources (e.g., lunar regolith) and high-performance terrestrial materials. In this context, laser additive manufacturing of metallic lattice structures not only advances aerospace propulsion and thermal management applications but also emerges as a transformative enabler for extraterrestrial habitat protection, underscoring its broad relevance to future space exploration.

The James Webb Space Telescope (JWST) sunshield support system underscores the critical importance of lightweight, dimensionally stable architectures in space applications. While existing literature does not explicitly describe these supports as "lattice structures", their multilayer, low-mass, and high-stiffness framework reflects design philosophies that parallel those of metallic lattices fabricated by laser additive manufacturing [111,112]. Both approaches leverage carefully engineered geometries and advanced materials—whether high-modulus composites, beryllium, or additively manufactured alloys to suppress thermal deformation and maintain precision alignment under extreme temperature gradients of up to 300 K [111,112]. This analogy illustrates how the core principles underpinning lattice design, lightweighting, multifunctionality, and structural stability are already validated in flagship aerospace missions. Extending these concepts through laser additive manufacturing of metallic lattices could further enable thermally stable, load-bearing components for next-generation space telescopes and satellites, thereby reinforcing the broader relevance of lattice-enabled architecture across aerospace and space exploration.

10. Challenges and future perspectives

10.1. Challenges and limitations

Surface roughness remains a persistent challenge, with *Ra* values typically 10–20 μm for as-built surfaces [113]. While post-processing improves surface quality, accessibility within complex lattice geometries limits effectiveness. Chemical etching shows promise but requires careful control to prevent strut thinning [114]. Table 1 summarizes the critical challenges and correlative solutions. Size limitations constrain industrial adoption. Current SLM systems accommodate maximum build volumes of 500 × 500 × 500 mm^3, insufficient for large aerospace components [115]. Multi-laser systems and hybrid manufacturing approaches offer potential solutions but introduce additional complexity [116].

Material limitations restrict design freedom. The requirement for spherical powder morphology and the limited number of alloy systems compatible with LAM constrain material selection [117]. The development of new alloys specifically designed for AM processing is an active research area [118]. Manufacturing yield and consistency remain industrial concerns, with typical first-pass success rates of 70%–85% for complex lattice geometries due to support failure, distortion, or defect formation. Quality variation between machines and even within build plates can be significant, driving investment in real-time monitoring and adaptive control systems.

Residual stress accumulation poses another critical limitation, particularly for complex lattice geometries. Unlike solid components, where heat dissipates in all directions, the thin struts of lattice architectures restrict thermal conduction paths, leading to localized heat accumulation and severe thermal gradients. This mismatch often results in geometric distortion or even strut separation. Support structures, therefore, must serve a dual function: providing mechanical anchoring and acting as essential thermal conduits to facilitate heat dissipation to the build plate.

10.2. Emerging opportunities

Machine learning integration throughout the design-manufacture-test cycle promises transformative capabilities [119]. Generative design algorithms explore vast design spaces, identifying non-intuitive solutions exceeding human-designed performance by 30%–40% [120]. Reinforcement learning optimizes process parameters in real time, adapting to material and machine variations [121]. Multi-material and functionally graded structures enable unprecedented combinations of properties. Recent developments in multi-nozzle systems enable material switching within a single layer, creating true 3D composition variation [122]. This capability enables simultaneous optimization of multiple properties (strength, conductivity, density) [123]. Sustainability considerations drive the development of recycled powder utilization and reduced energy consumption. Closed-loop powder recycling systems maintain powder quality through 20+ reuse cycles [124]. Process optimization that reduces energy consumption by 40% while maintaining part quality demonstrates environmental responsibility [125].

10.3. Future research directions

Understanding fundamental mechanisms governing defect formation requires advanced characterization. *In-situ* synchrotron studies with microsecond temporal resolution reveal the dynamics of solidification and defect nucleation [126]. These insights inform physics-based process models for defect prediction and prevention [127]. The development of lattice-specific design tools that integrate manufacturing constraints, performance requirements, and cost considerations remains critical. Cloud-based platforms enabling collaborative design and simulation accelerate development cycles [128]. Integration with digital twin frameworks enables lifecycle performance prediction and optimization [123]. Qualification and certification procedures specific to lattice structures need to be developed. Statistical approaches that account for spatial property variation and defect distributions provide a robust design. Machine learning-based quality prediction reduces testing requirements while maintaining safety margins [129,130].

Table 1. Critical challenges and current solutions.

Challenges	Current solutions	Effectiveness	References
Surface roughness (Ra 15–25 μm)	Chemical etching, electropolishing	40%–60% improvement	[114,115]
Size limitations (500 × 500 × 500 mm^3)	Multi-laser systems, hybrid manufacturing	Partial solution	[116,117]
Residual stress	Optimized scanning, preheating, HIP	70%–90% reduction	[16,86]
Material limitations	AM-specific alloy development	Ongoing research	[118,119]
Qualification standards	ASTM/ISO standard development	Emerging framework	[130]
Production consistency	AI-based monitoring, closed-loop control	85%–95% yield improvement	[55,95]

11. Conclusion

Laser additive manufacturing has profoundly transformed the fabrication of metallic lattice structures, offering unprecedented design flexibility and the ability to achieve unique property combinations. Over the past decade, advances have spanned the full ecosystem from material development and structural design to process understanding, property evaluation, and industrial application. Material innovations now extend well beyond conventional alloys, incorporating composites and functionally graded systems

in which *in-situ* alloying and reinforcements unlock new performance possibilities. On the design side, methodologies have evolved from simple periodic lattices to sophisticated hierarchical and gradient architectures, increasingly optimized using computational tools such as machine learning and topology optimization. Parallel advances in process monitoring and modelling, aided by high-speed imaging, have shed light on the mechanisms governing defect formation and microstructure evolution. These insights are complemented by mechanical characterizations that demonstrate how architecture can tailor responses, though challenges remain in fully understanding fatigue and fracture behavior.

The integration of multifunctional capabilities, such as structural, thermal, and dynamic, has further underscored the potential of lattices for system-level optimization and weight reduction. Meanwhile, quality assurance has advanced significantly, with automated defect detection and *in-situ* monitoring nearing industrial maturity. However, critical barriers persist, particularly regarding surface quality, large-scale fabrication, and certification standards. Looking ahead, research must deepen the physics-based understanding of process-structure-property linkages, create lattice-specific design and analysis frameworks, and establish robust qualification pathways for safety-critical applications. The convergence of advanced materials, intelligent design tools, and high-precision manufacturing systems positions metallic lattice structures as a cornerstone technology for next-generation aerospace and beyond, provided continued investment sustains the pace of fundamental and applied innovations.

Declaration of generative AI and AI-assisted technologies

During the preparation of this manuscript, the authors used generative AI tools only to improve language and readability. The authors take full responsibility for the content of the manuscript.

Acknowledgments

The authors would like to acknowledge the Ministry of Education Malaysia: FRGS/1/2023/TK10/UMP/02/9 for funding this research. This work is strongly supported by the Structural Performance Materials Engineering (SUPREME) Focus Group.

Authors' contribution

Bo Sun: methodology, investigation, writing—original draft; Shixun Zheng: literature review, data curation; writing–review & editing; Haoyu Liu: writing—review & editing; Sharifah Fatmadiana Wan Muhamad Hatta: supervision of additive manufacturing-related content; Binghua Yang: contributions to materials science and microstructural evolution sections; Zhaoji Zong: support in numerical modeling and quality control discussions; Quanjin Ma: supervision, writing—review & editing. All authors reviewed and approved the final version of the manuscript.

Conflicts of interest

The authors declare no conflicts of interest.

References

[1] Chen L, Liang S, Liu Y, Zhang L. Additive manufacturing of metallic lattice structures: Unconstrained design, accurate fabrication, fascinated performances, and challenges. *Mater. Sci. Eng.: R: Rep.* 2021, 146:100648.

[2] Kumar A, Collini L, Daurel A, Jeng J. Design and additive manufacturing of closed cells from supportless lattice structure. *Addit. Manuf.* 2020, 33:101168.

[3] Maconachie T, Leary M, Lozanovski B, Zhang X, Qian M, *et al.* SLM lattice structures: properties, performance, applications and challenges. *Mater. Des.* 2019, 183:108137.

[4] Zhang M, Yang Y, Wang D, Song C, Chen J. Microstructure and mechanical properties of CuSn/18Ni300 bimetallic porous structures manufactured by selective laser melting. *Mater. Des.* 2019, 165:107583.

[5] DebRoy T, Wei H, Zuback JS, Mukherjee T, Elmer JW, *et al.* Additive manufacturing of metallic components–process, structure and properties. *Prog. Mater Sci.* 2018, 92:112–224.

[6] Herzog D, Seyda V, Wycisk E, Emmelmann C. Additive manufacturing of metals. *Acta Mater.* 2016, 117:371–392.

[7] Schaedler TA, Carter WB. Architected cellular materials. *Annu. Rev. Mater. Res.* 2016, 46(1):187–210.

[8] Thompson MK, Moroni G, Vaneker T, Fadel G, Campbell RI, *et al.* Design for additive manufacturing: trends, opportunities, considerations, and constraints. *CIRP Ann.* 2016, 65(2):737–760.

[9] Panesar A, Abdi M, Hickman D, Ashcroft I. Strategies for functionally graded lattice structures derived using topology optimisation for additive manufacturing. *Addit. Manuf.* 2018, 19:81–94.

[10] Wohlers T. Wohlers Report 2020: 3D printing and additive manufacturing global state of the industry. 2020. Available: https://wohlersassociates.com/2020report.htm (accessed on 11 April 2026).

[11] Khairallah SA, Anderson AT, Rubenchik A, King WE. Laser powder-bed fusion additive manufacturing: physics of complex melt flow and formation mechanisms of pores, spatter, and denudation zones. *Acta Mater.* 2016, 108:36–45.

[12] Yadroitsev I, Krakhmalev P, Yadroitsava I. Hierarchical design principles of selective laser melting for high quality metallic objects. *Addit. Manuf.* 2015, 7:45–56.

[13] Seifi M, Gorelik M, Waller J, Hrabe N, Shamsaei N, *et al.* Progress towards metal additive manufacturing standardization to support qualification and certification. *Jom* 2017, 69(3):439–455.

[14] Reed RC. *The Superalloys: Fundamentals and Applications*. Cambridge: Cambridge University Press, 2008.

[15] Hosseini E, Popovich VA. A review of mechanical properties of additively manufactured Inconel 718. *Addit. Manuf.* 2019, 30:100877.

[16] Zhang M, Sun CN, Zhang X, Goh PC, Wei J, *et al.* Fatigue and fracture behaviour of laser powder bed fusion stainless steel 316L: influence of processing parameters. *Mater. Sci. Eng. A* 2017, 703:251–261.

[17] Chen Y, Clark SJ, Huang Y, Sinclair L, Leung C, *et al. In situ* X-ray quantification of melt pool behaviour during directed energy deposition additive manufacturing of stainless steel. *Mater. Lett.* 2021, 286:129205.

[18] Trosch T, Strößner J, Völkl R, Glatzel U. Microstructure and mechanical properties of selective laser melted Inconel 718 compared to forging and casting. *Mater. Lett.* 2016, 164:428–431.

[19] Briones-Montemayor MJ, Guzmán-Nogales R, Majari P, Estrada-Díaz JA, Elías-Zúñiga A, *et al.* Enhanced mechanical performance of SLM-printed Inconel 718 lattice structures through heat treatments. *Metals* 2025, 15(7):686.
[20] Harrison NJ, Todd I, Mumtaz K. Reduction of micro-cracking in nickel superalloys processed by selective laser melting: a fundamental alloy design approach. *Acta Mater.* 2015, 94:59–68.
[21] Liu P, Wang Z, Xiao Y, Horstemeyer M, Cui X, *et al.* Insight into the mechanisms of columnar to equiaxed grain transition during metallic additive manufacturing. *Addit. Manuf.* 2019, 26:22–29.
[22] Liu S, Shin YC. Additive manufacturing of Ti6Al4V alloy: a review. *Mater. Des.* 2019, 164:107552.
[23] Xu W, Lui EW, Pateras A, Qian M, Brandt M. *In situ* tailoring microstructure in additively manufactured Ti-6Al-4V for superior mechanical performance. *Acta Mater.* 2017, 125:390–400.
[24] Wang D, Yang Y, Liu R, Xiao D, Sun J. Study on the designing rules and processability of porous structure based on selective laser melting (SLM). *J. Mater. Process. Technol.* 2013, 213(10):1734–1742.
[25] Ramadani R, Pal S, Belšak A, Predan J. Selective laser melting of a Ti-6Al-4V lattice-structure gear: design, topology optimization, and experimental validation. *Appl. Sci.* 2025, 15(14):7949.
[26] Zhang LC, Attar H. Selective laser melting of titanium alloys and titanium matrix composites for biomedical applications: a review. *Adv. Eng. Mater.* 2016, 18(4):463–475.
[27] Bermingham M, McDonald S, Dargusch M, StJohn D. Microstructure of cast titanium alloys. *Mater. Forum* 2007, 31:84–89.
[28] AlMangour B, Grzesiak D, Yang JM. Selective laser melting of TiB2/316L stainless steel composites: the roles of powder preparation and hot isostatic pressing post-treatment. *Powder Technol.* 2017, 309:37–48.
[29] Martin JH, Yahata BD, Hundley JM, Mayer JA, Schaedler TA, *et al.* 3D printing of high-strength aluminium alloys. *Nature* 2017, 549(7672):365–369.
[30] Li Y, Zhou J, Pavanram P, Leeflang M, Fockaert LI, *et al.* Additively manufactured biodegradable porous magnesium. *Acta Biomater.* 2018, 67:378–392.
[31] Wei C, Zhang Z, Cheng D, Sun Z, Zhu M, *et al.* An overview of laser-based multiple metallic material additive manufacturing: from macro-to micro-scales. *Int. J. Extreme Manuf.* 2020, 3(1):012003.
[32] Al-Ketan O, Al-Rub RK. Multifunctional mechanical metamaterials based on triply periodic minimal surface lattices. *Adv. Eng. Mater.* 2019, 21(10):1900524.
[33] Yang L, Yan C, Cao W, Liu Z, Song B, *et al.* Compression–compression fatigue behaviour of gyroid-type triply periodic minimal surface porous structures fabricated by selective laser melting. *Acta Mater.* 2019, 181:49–66.
[34] Zhang L, Song B, Fu J, Wei S, Yang L, *et al.* Topology-optimized lattice structures with simultaneously high stiffness and light weight fabricated by selective laser melting: design, manufacturing and characterization. *J. Manuf. Processes* 2020, 56:1166–1177.
[35] Plocher J, Panesar A. Review on design and structural optimisation in additive manufacturing: towards next-generation lightweight structures. *Mater. Des.* 2019, 183:108164.
[36] Choy SY, Sun CN, Leong KF, Wei J. Compressive properties of functionally graded lattice structures manufactured by selective laser melting. *Mater. Des.* 2017, 131:112–120.
[37] Zhang X, Fang G, Leeflang S, Zadpoor A, Zhou J. Topological design, permeability and mechanical behavior of additively manufactured functionally graded porous metallic biomaterials. *Acta Biomater.* 2019, 84:437–452.

[38] Meza LR, Zelhofer AJ, Clarke N, Mateos AJ, Kochmann DM, *et al.* Resilient 3D hierarchical architected metamaterials. *Proc. Natl. Acad. Sci.* 2015, 112(37):11502–11507.

[39] Zheng X, Lee H, Weisgraber TH, Shusteff M, DeOtte J, *et al.* Ultralight, ultrastiff mechanical metamaterials. *Science* 2014, 344(6190):1373–1377.

[40] Nashar M, Sutradhar A. Design of hierarchical architected lattices for enhanced energy absorption. *Materials* 2021, 14(18):5384.

[41] Dallago M, Winiarski B, Zanini F, Carmignato S, Benedetti M. On the effect of geometrical imperfections and defects on the fatigue strength of cellular lattice structures additively manufactured via selective laser melting. *Int. J. Fatigue* 2019, 124:348–360.

[42] Savio G, Rosso S, Curtarello A, Meneghello R, Concheri G. Implications of modeling approaches on the fatigue behavior of cellular solids. *Addit. Manuf.* 2019, 25:50–58.

[43] Park KM, Min KS, Roh YS. Design optimization of lattice structures under compression: study of unit cell types and cell arrangements. *Materials* 2021, 15(1):97.

[44] Liu L, Kamm P, García-Moreno F, Banhart J, Pasini D. Elastic and failure response of imperfect three-dimensional metallic lattices: the role of geometric defects induced by selective laser melting. *J. Mech. Phys. Solids.* 2017, 107, 160–184.

[45] Lozanovski B, Leary M, Tran P, Shidid D, Qian M, *et al.* Computational modelling of strut defects in SLM manufactured lattice structures. *Mater. Des.* 2019, 171:107671.

[46] Bidare P, Bitharas I, Ward R, Attallah M, Moore AJ. Fluid and particle dynamics in laser powder bed fusion. *Acta Mater.* 2018, 142:107–120.

[47] Mukherjee T, DebRoy T. A digital twin for rapid qualification of 3D printed metallic components. *Appl. Mater. Today* 2019, 14:59–65.

[48] Calta NP, Wang J, Kiss AM, Martin A, Depond PJ, *et al*. An instrument for *in situ* time-resolved X-ray imaging and diffraction of laser powder bed fusion additive manufacturing processes. *Rev. Sci. Instrum.* 2018, 89(5).

[49] Calignano F. Design optimization of supports for overhanging structures in aluminum and titanium alloys by selective laser melting. *Mater. Des.* 2014, 64:203–213.

[50] Gan MX, Wong CH. Practical support structures for selective laser melting. *J. Mater. Process. Technol.* 2016, 238:474–484.

[51] Leary M, Mazur M, Elambasseril J, McMillan M, Chirent T, *et al.* Selective laser melting (SLM) of AlSi12Mg lattice structures. *Mater. Des.* 2016, 98:344–357.

[52] Hussein A, Hao L, Yan C, Everson R. Finite element simulation of the temperature and stress fields in single layers built without-support in selective laser melting. *Mater. Des.* 2013, 52:638–647.

[53] Shevchik SA, Kenel C, Leinenbach C, Wasmer K. Acoustic emission for *in situ* quality monitoring in additive manufacturing using spectral convolutional neural networks. *Addit. Manuf.* 2018, 21:598–604.

[54] Hooper PA. Melt pool temperature and cooling rates in laser powder bed fusion. *Addit. Manuf.* 2018, 22:548–559.

[55] Grasso M, Colosimo BM. Process defects and *in situ* monitoring methods in metal powder bed fusion: a review. *Meas. Sci. Technol.* 2017, 28(4):044005.

[56] Everton SK, Hirsch M, Stravroulakis P, Leach RK, Clare AT. Review of *in-situ* process monitoring and *in-situ* metrology for metal additive manufacturing. *Mater. Des.* 2016, 95:431–445.

[57] Körner C. Additive manufacturing of metallic components by selective electron beam melting—a review. *Int. Mater. Rev.* 2016, 61(5):361–377.
[58] Ashby MF, Gibson LJ. *Cellular Solids: Structure and Properties.* Cambridge: Press Syndicate of the University of Cambridge, UK, 1997. pp. 175–231.
[59] Ashby MF. The properties of foams and lattices. *Philos. Trans. R. Soc. Ser. A* 2006, 364(1838):15–30.
[60] Gümrük R, Mines R. Compressive behaviour of stainless steel micro-lattice structures. *Int. J. Mech. Sci.* 2013, 68:125–139.
[61] Deshpande VS, Fleck NA, Ashby MF. Effective properties of the octet-truss lattice material. *J. Mech. Phys. Solids.* 2001, 49(8):1747–1769.
[62] Lee S, Barthelat F, Hutchinson JW, Espinosa HD. Dynamic failure of metallic pyramidal truss core materials—experiments and modeling. *Int. J. Plast.* 2006, 22(11):2118–2145.
[63] Tancogne-Dejean T, Spierings AB, Mohr D. Additively-manufactured metallic micro-lattice materials for high specific energy absorption under static and dynamic loading. *Acta Mater.* 2016, 116:14–28.
[64] Harris J, Winter R, McShane GJ. Impact response of additively manufactured metallic hybrid lattice materials. *Int. J. Impact Eng.* 2017, 104:177–191.
[65] McKown S, Shen Y, Brookes W, Sutcliffe C, Cantwell W, *et al.* The quasi-static and blast loading response of lattice structures. *Int. J. Impact Eng.* 2008, 35(8):795–810.
[66] Radford D, Deshpande V, Fleck N. The use of metal foam projectiles to simulate shock loading on a structure. *Int. J. Impact Eng.* 2005, 31(9):1152–1171.
[67] Dallago M, Raghavendra S, Luchin V, Zappini G, Pasini D, *et al.* Geometric assessment of lattice materials built via selective laser melting. *Mater. Today Proc.* 2019, 7:353–361.
[68] Benedetti M, Plessis A, Ritchie RO, Dallago M, Razavi N, *et al.* Architected cellular materials: a review on their mechanical properties towards fatigue-tolerant design and fabrication. *Mater. Sci. Eng.: R: Rep.* 2021, 144:100606.
[69] Zargarian A, Esfahanian M, Kadkhodapour J, Ziaei-Rad S. Numerical simulation of the fatigue behavior of additive manufactured titanium porous lattice structures. *Mater. Sci. Eng. C* 2016, 60:339–347.
[70] Hedayati R, Hosseini-Toudeshky H, Sadighi M, Mohammadi-Aghdam M, Zadpoor A. Computational prediction of the fatigue behavior of additively manufactured porous metallic biomaterials. *Int. J. Fatigue* 2016, 84:67–79.
[71] Maloney KJ, Fink KD, Schaedler TA, Kolodziejska JA, Jacobsen AJ, *et al.* Multifunctional heat exchangers derived from three-dimensional micro-lattice structures. *Int. J. Heat Mass Transfer* 2012, 55(9–10):2486–2493.
[72] Shen B, Yan H, Xue H, Xie G. The effects of geometrical topology on fluid flow and thermal performance in Kagome cored sandwich panels. *Appl. Therm. Eng.* 2018, 142:79–88.
[73] Liu J, Cheng D, Oo K, McCrimmon TL, Bai S. Design and additive manufacturing of TPMS heat exchangers. *Appl. Sci.* 2024, 14(10):3970.
[74] Catchpole-Smith S, Sélo R, Davis A, Ashcroft I, Tuck CJ, *et al.* Thermal conductivity of TPMS lattice structures manufactured via laser powder bed fusion. *Addit. Manuf.* 2019, 30:100846.
[75] Wong M, Owen I, Sutcliffe C, Puri A. Convective heat transfer and pressure losses across novel heat sinks fabricated by selective laser melting. *Int. J. Heat Mass Transfer* 2009, 52(1–2):281–288.

[76] Mueller J, Matlack KH, Shea K, Daraio C. Energy absorption properties of periodic and stochastic 3D lattice materials. *Adv. Theor. Simul.* 2019, 2(10):1900081.

[77] Matlack KH, Bauhofer A, Krödel S, Palermo A, Daraio C. Composite 3D-printed metastructures for low-frequency and broadband vibration absorption. *Proc. Natl. Acad. Sci.* 2016, 113(30):8386–8390.

[78] Krödel S, Thomé N, Daraio C. Wide band-gap seismic metastructures. *Extreme Mech. Lett.* 2015, 4:111–117.

[79] Wang Y, Wang Y, Wu B, Chen W, Wang Y. Tunable and active phononic crystals and metamaterials. *Appl. Mech. Rev.* 2020, 72(4):040801.

[80] Hussein MI, Leamy MJ, Ruzzene M. Dynamics of phononic materials and structures: historical origins, recent progress, and future outlook. *Appl. Mech. Rev.* 2014, 66(4):040802.

[81] Latture RM, Rodriguez RX, Holmes Jr LR, Zok FW. Effects of nodal fillets and external boundaries on compressive response of an octet truss. *Acta Mater.* 2018, 149:78–87.

[82] Cao X, Xiao D, Li Y, Wen W, Zhao T, *et al.* Dynamic compressive behavior of a modified additively manufactured rhombic dodecahedron 316L stainless steel lattice structure. *Thin-Walled Struct.* 2020, 148:106586.

[83] Hashin Z, Shtrikman S. A variational approach to the theory of the elastic behaviour of multiphase materials. *J. Mech. Phys. Solids.* 1963, 11(2):127–140.

[84] Raissi M, Perdikaris P, Karniadakis GE. Physics-informed neural networks: a deep learning framework for solving forward and inverse problems involving nonlinear partial differential equations. *J. Comput. Phys.* 2019, 378:686–707.

[85] Wang L, Chan YC, Liu Z, Zhu P, Chen W. Data-driven metamaterial design with laplace-beltrami spectrum as “shape-DNA”. *Struct. Multidiscip. Optim.* 2020, 61(6):2613–2628.

[86] Liang X, Dong W, Chen Q, To AC. On incorporating scanning strategy effects into the modified inherent strain modeling framework for laser powder bed fusion. *Addit. Manuf.* 2021, 37:101648.

[87] Bayat M, Thanki A, Mohanty S, Witvrouw A, Yang S, *et al.* Keyhole-induced porosities in laser-based powder bed fusion (L-PBF) of Ti6Al4V: high-fidelity modelling and experimental validation. *Addit. Manuf.* 2019, 30:100835.

[88] Cunningham R, Zhao C, Parab N, Kantzos C, Pauza J, *et al.* Keyhole threshold and morphology in laser melting revealed by ultrahigh-speed X-ray imaging. *Science* 2019, 363(6429):849–852.

[89] King WE, Barth HD, Castillo VM, Gallegos GF, Gibbs JW, *et al.* Observation of keyhole-mode laser melting in laser powder-bed fusion additive manufacturing. *J. Mater. Process. Technol.* 2014, 214(12):2915–2925.

[90] Plessis A, Yadroitsava I, Yadroitsev I. Effects of defects on mechanical properties in metal additive manufacturing: a review focusing on X-ray tomography insights. *Mater. Des.* 2020, 187:108385.

[91] Thompson A, Maskery I, Leach RK. X-ray computed tomography for additive manufacturing: a review. *Meas. Sci. Technol.* 2016, 27(7):072001.

[92] Zhang Y, Hong GS, Ye D, Zhu K, Fuh JY. Extraction and evaluation of melt pool, plume and spatter information for powder-bed fusion AM process monitoring. *Mater. Des.* 2018, 156:458–469.

[93] Gunasegaram DR, Murphy A, Barnard A, DebRoy T, Matthews M, *et al.* Towards developing multiscale-multiphysics models and their surrogates for digital twins of metal additive manufacturing. *Addit. Manuf.* 2021, 46:102089.

[94] Li J, Wang L, He X, Liang J, Dong C. Additively manufactured metallic TPMS lattice structures: design strategies, fabrication, multifunctional properties, and applications. *npj Adv. Manuf.* 2025, 2(1):45.

[95] Scime L, Beuth J. Anomaly detection and classification in a laser powder bed additive manufacturing process using a trained computer vision algorithm. *Addit. Manuf.* 2018, 19:114–126.

[96] Craeghs T, Clijsters S, Kruth JP, Bechmann F, Ebert MC. Detection of process failures in layerwise laser melting with optical process monitoring. *Physics Procedia* 2012, 39:753–759.

[97] Ye D, Hong GS, Zhang Y, Zhu K, Fuh JY. Defect detection in selective laser melting technology by acoustic signals with deep belief networks. *Int. J. Adv. Manuf. Technol.* 2018, 96(5):2791–2801.

[98] Maconachie T, Leary M, Tran P, Harris J, Liu Q, *et al.* The effect of topology on the quasi-static and dynamic behaviour of SLM AlSi10Mg lattice structures. *Int. J. Adv. Manuf. Technol.* 2022, 118(11):4085–4104.

[99] Torrents A, Schaedler T, Jacobsen A, Carter W, Valdevit L. Characterization of nickel-based microlattice materials with structural hierarchy from the nanometer to the millimeter scale. *Acta Mater.* 2012, 60(8):3511–3523.

[100] Pyka G, Kerckhofs G, Papantoniou I, Speirs M, Schrooten J, *et al.* Surface roughness and morphology customization of additive manufactured open porous Ti6Al4V structures. *Materials* 2013, 6(10):4737–4757.

[101] Gupta A, Bennett CJ, Sun W. High cycle fatigue performance evaluation of a laser powder bed fusion manufactured Ti-6Al-4V bracket for aero-engine applications. *Eng. Fail. Anal.* 2022, 140:106494.

[102] Najmon JC, Raeisi S, Tovar A. Review of additive manufacturing technologies and applications in the aerospace industry. *Addit. Manuf. Aerosp. Ind.* 2019, pp. 7–31.

[103] Dixit T, Al-Hajri E, Paul MC, Nithiarasu P, Kumar S. High performance, microarchitected, compact heat exchanger enabled by 3D printing. *Appl. Therm. Eng.* 2022, 210:118339.

[104] Zhang Y, Yang Y, Chen G, Jiang Q, Hao B. Analysis of the convective heat transfer performance of multi-morphology lattice structures in thermal management of high-speed aircraft. *Phys. Fluids* 2025, 37(1):015101.

[105] Uriondo A, Esperon-Miguez M, Perinpanayagam S. The present and future of additive manufacturing in the aerospace sector: a review of important aspects. *Proc. Inst. Mech. Eng., Part G: J. Aerosp. Eng.* 2015, 229(11):2132–2147.

[106] Xu L, Ruan Q, Shen Q, Xi L, Gao J, *et al.* Optimization design of lattice structures in internal cooling channel with variable aspect ratio of gas turbine blade. *Energies* 2021, 14(13):3954.

[107] Parbat S, Min Z, Yang L, Chyu M. Experimental and numerical analysis of additively manufactured inconel 718 coupons with lattice structure. *J. Turbomach.* 2020, 142(6):061004.

[108] Khan N, Riccio A. A systematic review of design for additive manufacturing of aerospace lattice structures: current trends and future directions. *Prog. Aerosp. Sci.* 2024, 149:101021.

[109] Kamareh F, Pang B, Cao W, Chi R, Hu D. Proposing novel body-centered cubic lattice core sandwich panels as satellite structure. *Adv. Space Res.* 2024, 74(11):5779–5802.

[110] Steiner JT, Malla RB. A study of layered structural configurations as thermal and impact shielding of lunar habitats. In *Proceedings of Earth and Space 2021*, Reston, USA, 2021, pp. 1285–1296.

[111] McElwain MW, Feinberg LD, Perrin MD, Clampin M, Mountain CM, *et al.* The James Webb Space Telescope Mission: optical telescope element design, development, and performance. *Publ. Astron. Soc. Pac.* 2023, 135(1047):058001.
[112] Mather JG, Clampin M. The James Webb Space Telescope. *Space Sci. Rev.* 2006, 123(4):485.
[113] Strano G, Hao L, Everson RM, Evans KE. Surface roughness analysis, modelling and prediction in selective laser melting. *J. Mater. Process. Technol.* 2013, 213(4):589–597.
[114] Pyka G, Burakowski A, Kerckhofs G, Moesen M, Van Bael S, *et al.* Surface modification of Ti6Al4V open porous structures produced by additive manufacturing. *Adv. Eng. Mater.* 2012, 14(6):363–370.
[115] Kruth JP, Levy G, Klocke F, Childs TH. Consolidation phenomena in laser and powder-bed based layered manufacturing. *CIRP Ann.* 2007, 56(2):730–759.
[116] Flynn JM, Shokrani A, Newman ST, Dhokia V. Hybrid additive and subtractive machine tools—research and industrial developments. *Int. J. Mach. Tools Manuf.* 2016, 101:79–101.
[117] Sutton AT, Kriewall CS, Leu MC, Newkirk JW. Powder characterisation techniques and effects of powder characteristics on part properties in powder-bed fusion processes. *Virtual Phys. Prototyping* 2017, 12(1):3–29.
[118] Pollock TM, Tin S. Nickel-based superalloys for advanced turbine engines: chemistry, microstructure and properties. *J. Propul. Power* 2006, 22(2):361–374.
[119] Jiang J, Xiong Y, Zhang Z, Rosen DW. Machine learning integrated design for additive manufacturing. *J. Intell. Manuf.* 2022, 33(4):1073–1086.
[120] Oh Y, Zhou C, Behdad S. Part decomposition and assembly-based (Re) design for additive manufacturing: a review. *Addit. Manuf.* 2018, 22:230–242.
[121] Wang C, Tan XP, Tor SB, Lim C. Machine learning in additive manufacturing: state-of-the-art and perspectives. *Addit. Manuf.* 2020, 36:101538.
[122] Bandyopadhyay A, Heer B. Additive manufacturing of multi-material structures. *Mater. Sci. Eng.: R: Rep.* 2018, 129:1–16.
[123] Loh GH, Pei E, Harrison D, Monzón MD. An overview of functionally graded additive manufacturing. *Addit. Manuf.* 2018, 23:34–44.
[124] Santecchia E, Spigarelli S, Cabibbo M. Material reuse in laser powder bed fusion: side effects of the laser—metal powder interaction. *Metals* 2020, 10(3):341.
[125] Kellens K, Mertens R, Paraskevas D, Dewulf W, Duflou JR. Environmental impact of additive manufacturing processes: does AM contribute to a more sustainable way of part manufacturing? *Procedia CIRP.* 2017, 61:582–587.
[126] Leung CL, Marussi S, Atwood RC, Towrie M, Withers PJ, *et al. In situ* X-ray imaging of defect and molten pool dynamics in laser additive manufacturing. *Nat. Commun.* 2018, 9(1):1355.
[127] Zhao C, Fezzaa K, Cunningham RW, Wen H, Carlo F, *et al.* Real-time monitoring of laser powder bed fusion process using high-speed X-ray imaging and diffraction. *Sci. Rep.* 2017, 7(1):3602.
[128] Bikas H, Stavropoulos P, Chryssolouris G. Additive manufacturing methods and modelling approaches: a critical review. *Int. J. Adv. Manuf. Technol.* 2016, 83(1):389–405.
[129] Seifi M, Salem A, Beuth J, Harrysson O, Lewandowski J. Overview of materials qualification needs for metal additive manufacturing. *Jom* 2016, 68(3):747–764.
[130] Yadollahi A, Shamsaei N. Additive manufacturing of fatigue resistant materials: challenges and opportunities. *Int. J. Fatigue* 2017, 98:14–31.